# A miniaturised balloon-borne cloud water sampler and its deployment in the high Arctic

Julika Zinke[1,2], Matthew Salter[1,2], Caroline Leck[2,3], Michael J. Lawler[4], Grace Porter[5], Michael Adams[5], Ian Brooks[5], Benjamin Murray[5], and Paul Zieger[1,2,*]

[1]Department of Environmental Sciences, Stockholm University, Stockholm, Sweden

[2]Bolin Centre for Climate Research, Stockholm University, Stockholm, Sweden

[3]Department of Meteorology, Stockholm University, Stockholm, Sweden

[4]Department of Chemistry, University of California, Irvine, California, USA

[5]School of Earth and Environment, University of Leeds, Leeds, United Kingdom

[*]Correspondence: paul.zieger@aces.su.se

Manuscript submitted to Tellus B, January 10, 2020

## Abstract

Poor understanding of aerosol-cloud interactions and cloud feedback processes in the Arctic climate system limit our ability to constrain future climate in the region and one important knowledge gap is the source of particles upon which cloud droplets and ice crystals have formed. If representative cloud-water can be obtained from Arctic clouds, it's chemical composition can be analysed to infer the sources of particles present within it. However, the balloon-borne active cloud water sampling systems required to obtain such samples have not previously been feasible due to their weight and the challenging environmental conditions. Here we present a miniaturised cloud-water sampler for balloon-borne collection of cloud water which was deployed during the Microbiology-Ocean-Cloud-Coupling in the High Arctic (MOCCHA) campaign in August and September 2018 along with the deployment protocol required to obtain representative samples

in the pristine conditions encountered. We present the chemical composition of the samples obtained as well as the ice-nucleating activity of the samples and discuss the implications of our results on aerosol-cloud interactions in the high Arctic.

# 1 Introduction

The climate in the Arctic is changing faster than in any other region. According to Serreze et al. (2007) near surface temperatures in the high Arctic are rising at a rate at least twice that of the global average and the Arctic sea ice is retreating in all seasons, most drastically in summer. While sea ice reflects incoming solar radiation, the ocean absorbs and stores solar radiation and releases the heat during autumn, warming the atmosphere and delaying the freeze up-period. By interacting with solar radiation, clouds can affect the Arctic surface radiation balance and thus the magnitude of Arctic amplification (Sedlar et al., 2011). The radiative properties of clouds are influenced by their chemical and physical properties (e.g. phase and drop size) as well as their altitude. The number of aerosols that are available to act as cloud condensation nuclei (CCN) for instance influences the brightness of a cloud (Twomey, 1977) while the life-time and phase of the cloud are impacted both by the number of CCN as well as ice-nucleating particles (INP) (Albrecht, 1989; Vergara-Temprado et al., 2018).

Because aerosols are relatively scarce in the high Arctic north of 80°N with concentrations that are usually lower than $100\,\mathrm{cm}^{-3}$ (Covert et al., 1996; Bigg et al., 1996), optically thin low-level stratus clouds with fewer but larger cloud droplets are very common (Curry and Ebert, 1992; Schweiger and Key, 1992) with cloud fractions as high as 80-90 % during summer (Tjernström et al., 2014). For regimes with very limited CCN concentrations (e.g. $< 10\,\mathrm{cm}^{-3}$) these clouds tend to warm the surface relative to clear conditions during most of the year, when surface reflectivity is higher than the cloud albedo and long-wave radiation processes dominate (Mauritsen et al., 2011). During the ice melt at the end of summer the surface reflectivity is reduced and clouds may thus have a cooling effect that influences the timing of the autumn freeze-up (Tjernström et al., 2014).

Those optically thin clouds are very sensitive to changes in aerosol conditions (Mauritsen et al., 2011; Stevens et al., 2018). For example, an increase in CCN due to climate change could increase

the albedo of the clouds (Twomey effect), increasing the cooling effect and possibly leading to decreased ice-melt (Leck et al., 2004). However, there remains insufficient understanding of the contribution of different aerosol sources in the Arctic to the population of CCN and ice nucleating particles (INP). The high Arctic generally has very low aerosol concentrations because it is distant from strong natural and anthropogenic sources and the clouds in this region tend to remove aerosol effectively (Leck et al., 1996). Hence, it is thought that CCN and INP from biological activity in the open ocean, marginal ice zone (MIZ) and open leads in the pack ice may play an important role (Leck et al., 2002; Leck and Bigg, 2005a,b).

During the International Arctic Ocean Expedition (IAOE-1991, Leck et al., 1996), Leck and Persson (1996b) observed that the oxidation products of dimethyl sulphide (DMS), such as sulphur dioxide ($SO_2$), sulphuric acid ($H_2SO_4$) and methane sulphonic acids (MSA) were important CCN precursors over the pack ice. Given that DMS is mainly produced in the MIZ (Leck and Persson, 1996a) where particle removal by cloud scavenging processes is important (Nilsson and Bigg, 1996), a local source of aerosols in the central Arctic Ocean was suspected. During the Arctic Ocean Expedition 1996 campaign (AOE-1996, Leck et al., 2001) very small aerosols with diameters $< 50$ nm that consisted mainly of polymer gels instead of $H_2SO_4$ (Leck and Bigg, 1999) were observed. During a subsequent Arctic Ocean Expedition (AOE-2001, Leck et al., 2004; Tjernström et al., 2004), it was observed that polymer gels similar to those found in the surface microlayer (SML) of open leads were present in the atmosphere near the surface (Leck and Bigg, 2005a,b). These polymer gels were excreted by bacteria, sea-ice algae and marine phytoplankton and consisted of water insoluble, heat resistant, highly surface active and highly hydrated polysaccharides that are often inter-bridged with divalent ions like calcium (Leck and Svensson, 2015; Orellana and Leck, 2015). During the Arctic Summer Cloud Ocean Study cruise (ASCOS, Tjernström et al., 2014) in summer 2008, Orellana et al. (2011) demonstrated that low-level cloud and fog droplets contained the same type of polymer gels found in open leads.

Despite evidence for a surface source of aerosols containing polymer gels, such a process may only be relevant for boundary layer (BL) clouds, where local sources in combination with upstream BL transport from the MIZ constitute the origin of CCN (Kupiszewski et al., 2013). In the free troposphere (FT), which is typically decoupled from the mixed BL through a strong inversion, the dominant aerosol source is likely to be long-range transport of aerosols advected

from continental regions. Nevertheless, the importance of long-range transported aerosols for the BL CCN and INP budget remains unclear. According to Kupiszewski et al. (2013) those aerosols advected long distances in the FT are not likely to be entrained into the BL and thus do not influence low-level stratiform cloud formation. However, Igel et al. (2017) argue that the FT is a potentially important source of aerosols to the BL through entrainment or by cloud-mediated transport through activation at cloud top and evaporation below cloud base. Igel et al. (2017) concluded that the potential importance of FT aerosols for the BL will be limited by a yet unknown frequency by which the FT aerosol will come in contact with the BL top. It is the unresolved nature of questions such as this and a general poor understanding of aerosol-cloud interactions and cloud feedback processes in the Arctic climate system that hinder improved projections of future climate in the Arctic.

Since the chemical composition of cloud water can be used to infer the sources of those particles upon which cloud droplets and ice crystals form, obtaining high quality cloud water samples is an important goal. As such, we set out to develop a new light-weight cloud water sampler. A key aim when developing the sampler was eventual deployment in elevated clouds on a tethered balloon during the Microbiology-Ocean-Cloud-Coupling in the High Arctic (MOCCHA) campaign in August and September 2018. Here, we present technical details of the instrument as well as results following analysis of the chemical composition of cloud water sampled in the high Arctic along with the propensity for these cloud water samples to nucleate as ice crystals.

# 2 Methods

## 2.1 The miniaturised cloud water sampler

The miniaturised cloud water sampler (mini-CWS) developed during this study is a single-stage cloud water collector based on the working principle of the Caltech active strand cloud water collector (CASCC2, Demoz et al., 1996). Within such samplers, cloud droplets are actively accelerated towards a heated sampling volume by a fan (we used the model DFB0912M from Delta Electronics, Taiwan), where they impact on Teflon strings. Following impaction on the strings, the cloud water is collected in a sampling bottle situated below the string cassette. The strings are inclined to enhance droplet removal through aerodynamic drag.

The mini-CWS uses six rows of heated Teflon strings for sample collection. The heating prevents excessive build-up of rime on the strings that could alter the collection efficiency. The cloud water is collected in acid-washed brown Nalgene plastic sampling bottles (NALG2004-0002, Thermo Fischer Scientific, USA) situated below the string cassette. The protocol for acid-washing is given in Table S1 in the supplementary material. Opaque Nalgene bottles were chosen to prevent break-down of compounds or changes of the biological activity in the samples by UV-radiation and because they were most suitable for analysis of inorganic ions with ion chromatography (IC). The mini-CWS is operated by three lithium batteries (K2 Laptop Powerbank 185 Wh / 50000 mAh, PowerOak, Netherlands) with a 12 V port to power the fan and a 20 V port to power the heating loop. The operating parameters of the mini-CWS are presented in Table 1 and a schematic of the mini-CWS is presented in Figure 1. A fin is attached to the rear of the instrument to ensure that the sampler is always aligned into the wind. A miniaturised optical fog sensor (mini-OFS, Sten Löfving Optical Sensors, Sweden) was used to measure the visibility. This measurement was used to estimate both the time spent inside cloud and the thickness of the cloud. The visibility sensor is sensitive for visibilities between 0-500 m; if the visibility exceeds 500 m, the output is limited to 5 V. In order to limit condensation on the receiver of the visibility sensor it was heated to a few degrees above ambient temperature. A low cost humidity and temperature sensor (TEMPerHUM RS485HUM, RDing Technology Limited Company, China) along with a GPS-antenna (GPM-03, Chang Hong Technology Co Ltd, Taiwan) were connected to a computer (Raspberry Pi 3 model B, United Kingdom) to record temperature, humidity and location. An example of the data recorded during deployment can be seen in Figure S2 in the supplementary material. A timer (LT4H-W, Panasonic, Japan) was used to automatically switch between each active sampling period using the fan and the heating period. During each heating period the fan was switched off to minimise evaporation.

The droplet size sampling efficiency of the mini-CWS was estimated using the approach of Demoz et al. (1996). As can be seen in Figure 2a, the 50% cut size, which is the droplet aerodynamic diameter collected with 50% efficiency, lies at around 8 µm and the maximum efficiency of around 70% is reached at approximately 10 µm. Factors that impact the collection efficiency are the surface area of the strings, the ratio of the cross-sectional area of the strings in a row to the cross sectional area of the sampler, the number of rows as well as the turbulence of the flow which is

dependent on the air speed, air viscosity, strand diameter, droplet diameter (and density) and the angle of inclination of the strings. An increase in strand diameter (for instance through rime accumulation) can potentially increase the collection efficiency. In addition to this, an increase in flow speed, e.g. through additional horizontal wind, can cause cloud droplets with smaller diameters to be sampled more efficiently (see Figure 2b). The volume of cloud water likely to be obtained during a typical deployment in the high Arctic was estimated by multiplying the collection rate for different cloud liquid water contents (LWC, for a more detailed derivation see Demoz et al., 1996) with the sampling time. Since the Arctic atmosphere is rather dry (Kumai, 1973) the LWC was expected to remain below $0.1\,\mathrm{gm}^{-3}$. Given these conditions the sampler was expected to yield a sample volume of slightly less than 20 mL for a sampling period of approximately 5 hours (see Figure S1b in the supplementary material).

## 2.2 Deployment of the cloud water sampler in the high Arctic

The mini-CWS was deployed during the Microbiology-Ocean-Cloud-Coupling in the High Arctic (MOCCHA) campaign which took place in summer and early fall, 2018 close to the geographic North pole. The campaign had the primary goal of studying the life cycle of the high Arctic low-level clouds and was part of the US-Swedish Arctic Ocean 2018 expedition on board the Swedish icebreaker *Oden*. For five weeks, the icebreaker was moored to an ice floe upon which an ice camp was installed. The mini-CWS was operated from a tethered balloon (SkyHook helikite, Allsopp Helikites Ltd, United Kingdom) installed on the ice floe. The collection altitude of the samples, the sampling locations, the sampling times along with details of the analytical techniques subsequently applied to each sample are provided in Table S4 in the supplementary material.

All samples were bulk cloud water samples which were collected over several hours. The time in cloud was estimated for each deployment using the measured visibility. A visibility below 500 m was used as a threshold for determining when the instrument was within a cloud. During two deployments, the batteries were fully discharged before the sampler was retrieved and as such the exact time spent in cloud is unknown. However, the measured times in cloud are still given in such cases, since they allow an estimate of the active sampling time within cloud. It is important to note though that those samples collected when the batteries were fully discharged

may have been influenced by ice growth via condensation of water directly on the strings. As can be seen from Table S4, the rate of sample collection varied significantly across the different deployments. In some cases very little sample was obtained, even though the sampler was in cloud for several hours, while other samples with higher volumes were obtained in a very short period of time. This highlights the influence of factors other than the sampler parameters on the obtained sample volume such as the cloud LWC. In addition, it can not be excluded that icing on the strings as well as precipitation (e.g. blowing snow) might have contributed to the cloud water samples obtained.

### 2.2.1 Sample handling

Following each deployment, the sample bottle was immediately returned to the ship where it was weighed in order to determine the volume of cloud water sampled. Depending on the volume of cloud water sampled, subsamples were transferred into pre-cleaned plastic tubes that were acid-washed, using acid-washed plastic pipettes and analysed immediately.

To avoid contamination, the cloud water sampler was cleaned rigorously prior to each deployment. The cleaning process was designed to minimise contamination by inorganic ions, organic matter and bacteria, since these fractions were the subject of later analysis. Further, since the concentration of inorganic ions, organic matter and bacteria in the cloud water samples obtained was expected to be very low, an estimate of the background contamination originating from the sampler itself was required. To facilitate this estimate, handling blanks were obtained by collecting ultrapure deionised water (Millipore Alpha-Q, MQ, with a resistivity of 18 MΩcm at 25°C) using the sampler. To achieve this, an acid-washed spray bottle was used to spray the sampler strings with the ultrapure deionised water. Along with these handling blanks, the same ultrapure deionised water used to fill the spray bottle was also analysed before and after entering the spray bottle. This approach was used to exclude contamination of the water itself or of the spray bottle.

Acid-washing is usually used to remove contamination by organic matter. However, this approach could not be utilised to clean the mini-CWS, since the mounting of the strings contained metal parts and the funnel was entirely made of brass, which both are very reactive with acids. As such, a series of different cleaning procedures were tested to determine their efficiency for

removing contamination. Following each of the approaches a new handling blank was obtained and subsequently analysed for its chemical composition or propensity to nucleate ice. A detailed overview of each the cleaning approaches used along with their respective handling blanks is given in Table S2 in the supplementary material.

As a result of this testing the following cleaning procedure of the strings and metal parts of the sampler was found to be optimal. Firstly, a rinse with ethanol (95% analytical grade, Solveco, Sweden) was used to remove organic matter contamination from both the strings and the metal parts of the sampler (e.g. the sampling funnel). Secondly, UV irradiation of the strings was applied to reduce contamination by bacteria. For this, the strings were irradiated for 20 minutes on each side in a vertical-laminar air flow cabinet (Mini V/PCR, Telstar, Spain) with a TUV 30W 1SL/25 UV-lamp (Philips, Netherlands). Finally, the string cassette and funnel were rinsed with MQ water in an ultrasonic bath to remove remaining inorganic contaminants before being dried with particle free air/nitrogen in the laboratory.

The handling blanks collected during the expedition were compared with post-cruise instrumental blanks that were collected in the lab using the same cleaning procedures as described in Table S2 and the same equipment as during the campaign. Despite our attempts to recreate the same sampling conditions experienced during the expedition it is impossible for us to rule out that sources of contamination may have existed during the campaign that were not present during our later blank testing in the lab. The results of the comparison are discussed in Section 3.1.

### 2.2.2 Ion chromatography

An ICS-2000 ion chromatography system (Thermo Fischer Scientific, previously Dionex) was used to determine the concentration of the major anions and cations in the samples. The anions were analysed using a Dionex AG11 pre-column and a Dionex AS11 main column and the cations were analysed using a CG16 pre-column and a CS16 main-column. A Dionex ATC-1 column was used before the injection valve to trap carbonates and other ionic contaminants. Quality checks were performed using internal reference samples. Systematic errors were less than 2% for all ionic components with the exception of magnesium, $Mg^{2+}$, with less than 3% and the overall analytical accuracy was better than 3% and 5% for the anions and cations, respectively. The

detection limit was defined when the signal exceeded two standard deviations of the noise and was found to be 0.2, 0.05, 0.01, 0.005, 0.005, 0.05, 0.00, 0.02 and 0.005 $\mu molL^{-1}$ for ammonium ($NH_4^+$), sodium ($Na^+$), potassium ($K^+$), $Mg^{2+}$, calcium ($Ca^{2+}$), chloride ($Cl^-$), MSA ($CH_3SO_3^-$), nitrate ($NO_3^-$) and sulphate ($SO_4^{2-}$) respectively, according to the method of Leck and Svensson (2015). The limits of quantification are usually defined as twice the measured values in handling blanks, but were found to be dependent on the amount of rinsing with deionised water during cleaning in this study.

### 2.2.3 Thermal desorption chemical ionisation mass spectrometry

The chemical composition of a subset of cloud water samples were analysed using thermal desorption chemical ionisation mass spectrometry (TDCIMS). To do so, a 1 µL droplet of the sample was applied to a platinum filament where it was dried for $\sim$ 120 seconds before the filament was translated into the ion source of the mass spectrometer, which was filled with high purity nitrogen gas (AGA Detektor 5.5). Subsequently the filament temperature was ramped to about 800°C during 45 seconds to volatilise the collected mass from the wire. The desorbed molecules and pyrolysis fragments were ionised through reaction with the reagent ions and detected using a high-resolution time-of-flight mass spectrometer (TofWerk AG, Switzerland). The TDCIMS is capable of detecting both positive and negative ions, where $(H_2O)_nH_3O^+$ is the reagent for positive mode and $(H_2O)_nO_2^-$ for the negative mode (Lawler et al., 2014). The samples and handling blanks were diluted ten times before they were run in negative mode, because the signal was too high otherwise. Ultrapure water was also analysed using the same approach to assess the instrument background. A detectable signal was defined if the background-corrected signals were two standard errors above background (Lawler et al., 2014). For the estimation of the signal error see Lawler et al. (2014).

### 2.2.4 Ice nucleating particle analysis

The cloud water samples were also investigated for their propensity to nucleate ice crystals. For the INP analysis, a microlitre Nucleation by Immersed Particle Instrument (µL-NIPI, see Whale et al., 2015) was used. Around 40 droplets with a volume of 1 µL of each sample were placed on a 22 mm diameter hydrophobic silanised glass slide of 0.22 mm thickness (HR3-231,

Hampton Research, USA) using an electronic pipette (Picus Biohit, Sartorius, Germany) with an uncertainty of $\pm 0.025\,\mu$L. The slide was cleaned with ethanol, isopropanol and MQ water prior to the experiment. The pipetting was conducted with the glass slide placed on a cold stage (EF600, Grant-Asymptote, United Kingdom) and the slide was subsequently enclosed within a Perspex chamber while a flow of dry zero-grade nitrogen ($0.2\,\mathrm{L min^{-1}}$) was passed through the cell in order to prevent frost growth (Whale et al., 2015). The temperature of the plate was decreased at a constant rate of 1°C per minute and a digital camera (Lifecam HD, Microsoft, USA) recorded the state of the droplets each second. The temperature at which the drops begin to freeze provides insight into the type of INPs present in the sample. The maximum temperature error was estimated to be $\pm 0.4$°C (Whale et al., 2015). The cumulative concentration of INP (per unit volume of cloud water) on cooling was determined from the fraction of droplets frozen using the approach set out in Whale et al. (2015). To assess whether protein based INPs were present in the cloud water samples some of the samples were heated to 100°C for 30 minutes prior to analysis (O′Sullivan et al., 2018). To reduce the possibility of changes in the samples, they were stored in a fridge at about 5°C for no more than 48 hours before analysis. Further, freezing of the samples prior to analysis was avoided.

### 2.3 Back-trajectory analysis

Air mass back-trajectories were used to estimate the origin of air masses for the periods during which the mini-CWS was sampling. We have obtained 5-day back-trajectories calculated using the Lagrangian analysis tool LAGRANTO (Sprenger and Wernli, 2015) and wind fields from 3-hourly operational ECMWF analyses, starting at the ships position at 25 vertical levels. The vertical levels span between 0 and 500 hPa below sea level pressure. The LAGRANTO model also provides estimates of the BL depth, precipitation amount and other meteorological parameters along each trajectory.

# 3 Results

## 3.1 Assessment of background contamination

Since the concentrations of inorganic and organic ions as well as INPs were expected to be very low over the pack ice, emphasis had to be put on the development of a suitable cleaning procedure to minimise background contamination through the sampler.

Figure 3a compares the inorganic ion concentrations in the handling blanks with concentrations in the post-cruise instrumental blanks as well as concentrations in ultrapure MQ water, bottle blanks and spray bottle blanks. It is shown that neither the MQ water nor the sampling or spray bottle are significant sources of contamination. It can be clearly seen that the first handling blank collected on *Oden* had substantially higher concentrations than the instrumental blank with the same applied cleaning procedure. However, it should be considered that no sample was taken between the collection of the instrumental blanks and the sampler was therefore not exposed to as high levels of contamination as during the expedition in the Arctic. Nonetheless, the concentrations in the first handling blank are also substantially higher than in the succeeding handling blanks which compare reasonably well to the instrumental blanks (see Figure S4 in the supplementary material). This is probably due to contamination resulting from packing and shipping, since it was the first blank to be collected after unpacking of the instrument. Furthermore, residual dirt from the welding was found in the weld seams which was removed after thorough cleaning in the succeeding cleaning procedures. In future versions of the mini-CWS we plan to replace the brass funnel by a stainless steel version to reduce the contamination by the sampler itself.

From Figure 3b it becomes clear that the level of background contamination was almost exponentially decreasing with the number of rinses with ultrapure MQ water. After six rinses the concentrations were reasonably low (less than 10% compared to concentrations in the samples for all inorganic ions except $Ca^{2+}$ considering the first two cleaning procedures and only 1% for the final cleaning procedure CPIII). In fact, the number of rinses seems to be even more important for removing the inorganic background contamination than the different cleaning procedures that were applied. Further it must be noted that the contamination seemed to be time dependent. We suspect static deposition of aerosols from the room air to be a source of con-

tamination on the strings of the sampler and would therefore recommend deploying the sampler immediately after cleaning (or to store it in a clean room / glove box) to minimise contamination on the strings by room air.

### 3.2 Chemical composition

The amount of sampled cloud water was often very low to the extent that sufficient sample volume for each of the different analysis techniques was rarely available. While the INP measurements and thermal desorption chemical ionisation mass spectrometry only required a few microlitres of sample volume, the ion chromatography required at least 2.5 mL. Given these constraints, we were unable to apply all available analytical methods to each of the cloud water samples. An overview of the techniques applied to each sample collected during the expedition is given in Table S4. It should be noted that all the analysis discussed here was performed on the ship during the expedition (except for the post-cruise blanks).

Figure 4 shows the fractions and mole concentrations of the measured anions and cations obtained from IC analysis of the cloud water samples (before being corrected by the blank concentrations) that were collected on 17 August, 22 August, 25 August and 11 September compared to their respective handling blanks. It can be seen that the concentrations varied substantially between the samples and were in most cases dominated by the high concentrations of $Na^+$ and $Cl^-$, which most likely originated from primary sea spray particles. The sample collected on 17 August contained a significant amount of $NO_3^-$, $SO_4^{2-}$, MSA, $K^+$ and $Ca^{2+}$ that can be distinguished from the high concentrations in the handling blank (see Figure 4, ratio of blank concentrations to sample concentrations are given in Table S3 in the supplementary material). All concentrations discussed below have been corrected by the concentrations in the respective handling blanks. The presence of $SO_4^{2-}$, MSA and $Ca^{2+}$ indicates a marine source of aerosol. The sulphate may be present in the form of primary sea spray or may be the result of the atmospheric oxidation of DMS. With DMS oxidation being the only source of MSA, MSA is an important tracer for biogenic $SO_4^{2-}$ production (Karl et al., 2007). The concentrations of non-sea-salt-sulphate (nss-$SO_4$) can be calculated with the $Na^+$ concentration and sea water composition taken from Stumm and Morgan (1981): nss-$SO_4$ = $|SO_4| - (0.063 \cdot |Na|)$. The blank-corrected nss-$SO_4^{2-}$ concentrations were 7.6, 0.9, 0.8 and 2.7 $\mu molL^{-1}$ for the 17 August,

22 August, 25 August and 11 September, respectively. The molar ratio MSA/nss-$SO_4^{2-}$ (given in Table 2) can be used as a tracer for biological activity and indicates a marine source if MSA/nss-$SO_4^{2-} \geq 0.2$ (Leck and Persson, 1996b) which is true for all samples except the sample collected on 11 September, suggesting no biogenic contribution to this sample. The acidic $SO_4^{2-}$ can be partially or fully neutralised by reacting with ammonia to form ammoniated sulphate salts. The molar $NH_4^+$/nss-$SO_4^{2-}$ for 11 September was 1.29 indicating that the $SO_4^{2-}$ in this sample was partly neutralised.

The TDCIMS was most sensitive to contamination and therefore detected high background levels in the blanks even when the other methods did not. The blank sample that was collected on 28 August was the first to be considered clean in the TDCIMS, which is why only samples collected after this handling blank are discussed below. Figure 5 displays the detected ions in the blank sample and the cloud water samples that were collected after the final cleaning procedure was established. Only the sample collected on 11 September was analysed both with IC and TDCIMS. The sums of the detected ions were background-subtracted. The figure only contains anions with $\geq 1000$ ion counts and cations with $\geq 10000$ ion counts for the sake of clarity.

The negative ion spectra of the samples were dominated by fulminate ($CNO^-$), $Cl^-$, nitrite ($NO_2^-$), sulphur dioxide anions ($SO_2^-$) and iodide ($I^-$). The TDCIMS data appear to corroborate the high levels of salt detected in the IC analysis, with high levels of $Cl^-$ and $I^-$ in all samples. However, absolute signals of TDCIMS inorganic salt ions and organic ions cannot be used to infer relative ambient abundances of these species without calibration. In particular, electronegative species like I and $NO_2^-$ are detected more efficiently than most organics. The detected $SO_x^-$ ions are indicators for sulphur-containing salts. MSA was also detected. $I^-$ is known to originate from either $I^-$ or iodate ($IO_3^-$) salts and has been related to nucleation events in the past (Allan et al., 2015). The $NO_2^-$ ion is an indicator of $NO_3^-$ in the particles that might be of inorganic or organic origin. Nitrate was also found in the IC analysis of sample collected on 11 September, and TDCIMS-detected $NO_3^-$ was highest on this day, so a significant fraction may be inorganic.

The major positive ion species detected was $C_2H_5O^+$, which has been identified as acetaldehyde and detected in marine aerosol before by Lawler et al. (2014). They inferred it to be a decomposition product caused in the TDCIMS analysis of larger aldehydes, since it is too volatile to be a major component of small aerosol, but it may be produced in the decomposition of other gaseous

constituents as well. The salt cations $Na^+$ and $K^+$ were detected in all TDCIMS analyses. A very wide array of organic peaks were detected in positive ion mode. Many had desorption profiles consistent with semi-volatile secondary organic aerosol compounds, but there were also pyrolysis-derived peaks that likely arise from large molecules which may include primary marine aerosol. A substantial number of reduced nitrogen compounds are present in the positive ion mass spectrum. Many of these that are likely to be biogenic in origin, e.g. peaks consistent with urea ($C_4H_8N^+$) and phenylalanine ($C_9H_{12}NO_2^+$).

### 3.3 Ice-nucleating particle spectra

The droplet freezing assay allows the cumulative concentration of ice nucleating particles to be determined as a function of temperature. The cumulative concentrations of INP per litre of cloud water in the collected cloud water samples, handling blanks and MQ blanks are shown in Figure 6. Both samples and handling blanks started to freeze at higher temperatures than the respective MQ blanks, indicating that some contamination was introduced through the sampler. Only the samples collected on 24 and 25 August froze at temperatures that were considerably higher than the freezing temperatures of the handling blanks. The samples collected on 22 August and 11 September lie in or close to the baseline as set by the handling blanks. Therefore it is not possible to discern the INP content in these cloud water samples from the background contamination. In future deployments effort should be made to reduce the background contamination introduced by the sampler. In Figure 6 we also show the effect of heating the sample collected on the 25th August. Heating the sample shifts the curve to lower temperatures, indicating that the most active INP in the sample were destroyed by heating. This is consistent with the presence of protein based INP of biogenic origin (O′Sullivan et al., 2018). Terrestrial fungal and bacterial INP are both known to be sensitive to heat (Hill et al., 2016). INP associated with sea water have also been found to be heat sensitive (Schnell and Vali, 1975; Wilson et al., 2015; Irish et al., 2017). In contrast, inorganic INP such as mineral dusts are thought to be insensitive to heat (Hill et al., 2016; Conen et al., 2011).

In addition, we compare the INP concentrations we measured to measurements in precipitation and cloud water elsewhere in the world. Comparison with a compilation of INP concentrations in precipitation samples from around the world (Petters and Wright, 2015) shows that the two

days on which we had a clear signal, the concentrations were within the observed variability. We also note that our handling blanks define a limit roughly consistent with the lower bounds of the range defined by Petters and Wright (2015) which provides further motivation for future improvements in the approach used to clean the sampler. Comparison with other measurements of INP concentrations in cloud water in locations where mountains were available to access cloud altitudes are also shown. Three out of four samples are very similar to cloud water in Cape Verde (Gong et al., 2019), although the type of INP in the high Arctic is most likely very different to Cape Verde. In contrast the INP concentrations in the Arctic are shifted to lower temperatures compared to measurements in France (Joly et al., 2014). As a demonstration of the technique these results are highly valuable, but clearly more measurements are required to study the variability of INP in cloud water in the high-Arctic.

### 3.4 Source analysis and synthesis

In this section we want to synthesise the findings from the chemical and INP analysis with the trajectories of the collected samples. The sample collected on 17 August contained high concentrations of inorganic ions that indicated a marine source of aerosols. The trajectory analysis (see Figure 7) showed that the air on the 17 August originated from the Fram Strait, which was found to be a highly biologically productive area in previous studies (Leck and Persson, 1996a; Reigstad et al., 2011). Before arriving at the sampling site, most of the trajectories were within the BL and had spent roughly a day over the marginal ice zone (pack ice is only classified if the ice concentration exceeds 80%). Therefore, it might be possible that the cloud water concentrations of $SO_4^{2-}$ and MSA were derived by continuous photochemical DMS oxidation as the air was advected from the MIZ over the pack ice to the sampling site. This means that the molar ratio MSA/nss-$SO_4^{2-}$ observed at the ice floe is a result of both photochemically derived DMS oxidation products and their heterogeneous condensation on to pre-existing aerosol together with in cloud oxidation of $SO_2$ during a number of cloud cycles over the pack ice. This sample was excluded from INP analysis due to high levels of contamination in the handling blank.

The concentrations in the sample collected on 22 August were rather low compared to the other samples. The high molar ratio of $Cl^-/Na^+$ ($> 1.3$) indicates the presence of other cations

than $Na^+$ like $K^+$, $Ca^{2+}$ and $Mg^{2+}$. Before arriving at the sampling site, the air mass spent a significant amount of time over open water in the East Siberian Sea and Laptev Sea, which have been identified as biologically active regions in previous studies (Anderson et al., 2011) and which is consistent with the molar ratio MSA/nss-$SO_4^{2-}$ of 0.24. During the time over open water, all trajectories were below BL top, but precipitation occurred shortly before arrival at the sampling site, which might explain the low concentrations both in the IC and the INP analysis. However, precipitation also occurred along the trajectories for the samples collected on 24 and 25 August, which exhibited higher ice-nucleating activity. As discussed above, the heat sensitive INP in the sample collected on 25 August were suspected to be of biological origin. This is consistent with the high MSA/nss-$SO_4^{2-}$ ratio. Three out of four trajectories originated from Ellesmere Island. Surface based INP measurements at Alert on Ellesmere Island show that the concentrations are elevated in summer and autumn (Wex et al., 2019), suggesting there is a source of INP in this region. The trajectories on 11 September were similar to the trajectories on 25 August, but seemed to be confined to pack ice rather than the land. This could be an indication that the land is the key source of INP since INP concentrations in the sample collected on 11 September could not be discerned from the background contamination. Even though the trajectories on 11 September did not spend any time over open ocean and were above the BL top at all times, the sample still contained high salt concentrations ($Fl^-$ (fluoride), $Cl^-$, $Na^+$, $K^+$ and also some $Mg^{2+}$ and $Ca^{2+}$). These might have resulted from high winds upwind a frontal passage of the sampling site. However, one should keep in mind that trajectory calculations can still include large uncertainties (incl. depth of the BL and representation of decoupled clouds, Sotiropoulou et al., 2016) as they are based on re-analysis data which is especially uncertain for this region of the world.

# 4 Discussion

The collection of fog or cloud water for chemical analysis has been of great interest for many studies and a variety of active (size-resolved) cloud water collectors have been developed. Further, cloud water collection for chemical analysis has been performed under a range of conditions at several locations, e.g. at Mt. Rigi in Switzerland (Collett Jr et al., 1993), at Puy de Dôme

in France (Deguillaume et al., 2014) or at Mt. Schmücke in Germany (van Pinxteren et al., 2016) to name just a few of them. Figure 8 provides an overview of cloud water composition obtained from those studies compared with the findings of this study. All of the previous studies were limited to ground-based measurement sites in elevated mountain areas. To our knowledge, no balloon-borne active cloud water sampling has previously been performed in Arctic regions. Orellana et al. (2011) deployed a passive cloud sampler on a balloon, but this collection method involved ice growth by collision coalescence as well as deposition. The samples obtained in this study are bulk samples collected over several hours. While cloud droplets are sensitive to number concentrations, especially for smaller particles, the bulk property is dominated by the mass of potentially only a few large particles. As can be seen in Figure 8, the concentrations of the samples obtained in this study are substantially lower compared to the concentrations of the samples collected over central Europe, which is attributed to the remoteness of the central Arctic and limited influence from pollution sources during summer and early autumn.

# 5 Conclusion

A miniaturised cloud water sampler was developed for balloon-operated collection of cloud water. The newly developed sampler was able to retrieve bulk cloud water samples under the challenging Arctic conditions experienced during the Microbiology-Ocean-Cloud-Coupling in the High Arctic (MOCCHA) campaign in August and September 2018. The volumes that could be collected varied widely depending on time spent in cloud and the LWC of the cloud, but were also affected by riming or icing on the strings. The samples obtained were analysed by the same techniques used for aerosol measurements during the campaign which facilitates a later comparison of the ship-borne sampling of ambient aerosols and clouds. The composition of the analysed samples was found to vary substantially between the different samples and methods. Salts that probably originated from bubble bursting or breaking waves dominated the mole fractions obtained by IC analysis and were also observed in the TDCIMS spectra. Furthermore, oxidation products of DMS advected from the MIZ, were found. The INP analysis also points to the presence of cloud-forming particles of biological origin. However, definitive conclusions about the ice-nucleating activity of the samples cannot be made due to the relatively high ice-nucleating activity of the

measured handling blanks.

Future analysis of the samples will involve scanning electron microscopy, analysis of the amount and type of polysaccharides, proteins, sugars and fatty acids present, as well as DNA and bacteria analysis. With regards to further technical improvements of the sampler, future deployments in polar regions will require improvements to the heating system to better prevent ice formation within the sampler, which could never be fully avoided during sampling. Furthermore, the low-cost temperature and visibility sensors should be exchanged for sensors that are better adapted to very cold conditions to improve the determination of time spent in cloud.

## Acknowledgements

We thank Leif Bäcklin for his invaluable help in the construction of the instrument. We thank all helpers in the field, particularly Luisa Ickes, for their invaluable assistance and help. Linn Karlsson (ACES) is thanked for providing the data acquisition software. We gratefully acknowledge Emmy Nilsson (MISU) for invaluable assistance with the ion chromatography analysis. Heini Wernli (ETH Zürich, Switzerland) is acknowledged for providing the calculated trajectory data. We would like to extend our acknowledgement to Peggy Tesche-Achtert for providing the ceilometer data and the Atmospheric Measurement Facility of the British National Centre for Atmospheric Science for providing the ceilometer. The Swedish Polar Research (SPRS) provided access to the icebreaker *Oden* and logistical support. We are grateful to the SPRS logistical staff and to *Odens* Captain Mattias Peterson and his crew. This work was supported by the Swedish Research Council (grant no. 2016-03518, 2018-04255 and 2016-05100), the Swedish Research Council for Sustainable Development FORMAS (grant no. 2017-00567), the Knut-and-Alice Wallenberg Foundation (ACAS project, grant no. 2016.0024), the UK Natural Environment Research council (grant no. NE/R009686/1), the Bolin Centre for Climate Research at Stockholm University, as well as the European Research Council (ERC, MarineIce: grant no. 648661).

### Data availability

The data of this study will be made available on the data center of the Bolin Centre for Climate Research.

## References


Albrecht, B.A., 1989. Aerosols, cloud microphysics, and fractional cloudiness. *Science*, **245 (4923)**, 1227–1230.

Allan, J., Williams, P., Najera, J., Whitehead, J., Flynn, M., Taylor, J., Liu, D., Darbyshire, E., Carpenter, L., Chance, R. et al., 2015. Iodine observed in new particle formation events in the Arctic atmosphere during ACCACIA. *Atmospheric Chemistry and Physics*, **15 (10)**, 5599–5609.

Anderson, L.G., Björk, G., Jutterström, S., Pipko, I., Shakhova, N., Semiletov, I. and Wåhlström, I., 2011. East Siberian Sea, an Arctic region of very high biogeochemical activity. *Biogeosciences*, **8 (6)**, 1745–1754.

Bigg, K.E., Leck, C. and Nilsson, D.E., 1996. Sudden changes in arctic atmospheric aerosol concentrations during summer and autumn. *Tellus B*, **48 (2)**.

Brantner, B., Fierlinger, H., Puxbaum, H. and Berner, A., 1994. Cloudwater chemistry in the subcooled droplet regime at Mount Sonnblick (3106 m asl, Salzburg, Austria). *Water, Air, and Soil Pollution*, **74 (3-4)**, 363–384.

Collett Jr, J., Oberholzer, B. and Staehelin, J., 1993. Cloud chemistry at Mt Rigi, Switzerland: dependence on drop size and relationship to precipitation chemistry. *Atmospheric Environment. Part A. General Topics*, **27 (1)**, 33–42.

Conen, F., Morris, C., Leifeld, J., Yakutin, M. and Alewell, C., 2011. Biological residues define the ice nucleation properties of soil dust. *Atmospheric Chemistry and Physics*, **11 (18)**, 9643–9648.

Covert, D.S., Wiedensohler, A., Aalto, P., Heintzenberg, J., McMurry, P.H. and Leck, C., 1996.

Aerosol number size distributions from 3 to 500 nm diameter in the arctic marine boundary layer during summer and autumn. *Tellus B*, **48 (2)**.

Curry, J. and Ebert, E., 1992. Annual cycle of radiation fluxes over the arctic ocean: Sensitivity to cloud optical properties. *Journal of Climate*, **5 (11)**, 1267–1280.

Deguillaume, L., Charbouillot, T., Joly, M., Vaïtilingom, M., Parazols, M., Marinoni, A., Amato, P., Delort, A.M., Vinatier, V., Flossmann, A., Chaumerliac, N., Pichon, J.M., Houdier, S., Laj, P., Sellegri, K., Colomb, A., Brigante, M. and Mailhot, G., 2014. Classification of clouds sampled at the Puy de Dôme (France) based on 10 yr of monitoring of their physicochemical properties. *Atmospheric Chemistry and Physics*, **14 (3)**, 1485–1506.

Demoz, B., Collett, J. and Daube, B., 1996. On the Caltech Active Strand Cloudwater Collectors. *Atmospheric Research*, **41 (1)**, 47 – 62.

Gong, X., Wex, H., van Pinxteren, M., Triesch, N., Fomba, K.W., Lubitz, J., Stolle, C., Robinson, T.B., Müller, T., Herrmann, H. et al., 2019. Characterization of aerosol particles at Cape Verde close to sea and cloud level heights-part 2: ice nucleating particles in air, cloud and seawater. *Atmospheric Chemistry and Physics Discussion*.

Herenz, P., Wex, H., Mangold, A., Laffineur, Q., Gorodetskaya, I.V., Fleming, Z.L., Panagi, M. and Stratmann, F., 2019. CCN measurements at the Princess Elisabeth Antarctica research station during three austral summers. *Atmospheric Chemistry and Physics*, **19 (1)**, 275–294.

Hill, T.C.J., DeMott, P.J., Tobo, Y., Fröhlich-Nowoisky, J., Moffett, B.F., Franc, G.D. and Kreidenweis, S.M., 2016. Sources of organic ice nucleating particles in soils. *Atmospheric Chemistry and Physics*, **16 (11)**, 7195–7211.

Igel, A.L., Ekman, A.M., Leck, C., Tjernström, M., Savre, J. and Sedlar, J., 2017. The free troposphere as a potential source of arctic boundary layer aerosol particles. *Geophysical Research Letters*, **44 (13)**, 7053–7060.

Irish, V.E., Elizondo, P., Chen, J., Chou, C., Charette, J., Lizotte, M., Ladino, L.A., Wilson, T.W., Gosselin, M., Murray, B.J., Polishchuk, E., Abbatt, J.P.D., Miller, L.A. and Bertram, A.K., 2017. Ice-nucleating particles in Canadian Arctic sea-surface microlayer and bulk seawater. *Atmospheric Chemistry and Physics*, **17 (17)**, 10583–10595.

Joly, M., Amato, P., Deguillaume, L., Monier, M., Hoose, C. and Delort, A.M., 2014. Quantification of ice nuclei active at near 0° C temperatures in low-altitude clouds at the Puy de Dôme atmospheric station. *Atmospheric Chemistry and Physics*, **14 (15)**, 8185–8195.

Karl, M., Gross, A., Leck, C. and Pirjola, L., 2007. Intercomparison of dimethylsulfide oxidation mechanisms for the marine boundary layer: Gaseous and particulate sulfur constituents. *Journal of Geophysical Research: Atmospheres*, **112 (D15)**.

Kumai, M., 1973. Arctic fog droplet size distribution and its effect on light attenuation. *Journal of the Atmospheric Sciences*, **30 (4)**, 635–643.

Kupiszewski, P., Leck, C., Tjernström, M., Sjogren, S., Sedlar, J., Graus, M., Müller, M., Brooks, B., Swietlicki, E., Norris, S. et al., 2013. Vertical profiling of aerosol particles and trace gases over the central Arctic Ocean during summer. *Atmospheric Chemistry and Physics*, **13 (24)**, 12405–12431.

Lawler, M., Whitehead, J., O'Dowd, C., Monahan, C., McFiggans, G. and Smith, J., 2014. Composition of 15–85 nm particles in marine air. *Atmospheric Chemistry and Physics*, **14 (21)**, 11557–11569.

Leck, C. and Bigg, E., 1999. Aerosol production over remote marine areas - a new route. *Geophysical Research Letters*, **26 (23)**, 3577–3580.

Leck, C., Bigg, E., Covert, D., Heintzenberg, J., Maenhaut, W., Nilsson, E. and Wiedensohler, A., 1996. Overview of the atmospheric research program during the International Arctic Ocean Expedition of 1991 (IAOE-91) and its scientific results. *Tellus B*, **48 (2)**, 136–155.

Leck, C. and Bigg, E.K., 2005a. Biogenic particles in the surface microlayer and overlaying atmosphere in the central arctic ocean during summer. *Tellus B*, **57 (4)**, 305–316.

Leck, C. and Bigg, E.K., 2005b. Source and evolution of the marine aerosol - a new perspective. *Geophysical Research Letters*, **32 (19)**.

Leck, C., Nilsson, E.D., Bigg, E.K. and Bäcklin, L., 2001. Atmospheric program on the arctic ocean expedition 1996 (AOE-96): An overview of scientific goals, experimental approach, and instruments. *Journal of Geophysical Research: Atmospheres*, **106 (D23)**, 32051–32067.

Leck, C., Norman, M., Bigg, E. and Hillamo, R., 2002. Chemical composition and sources of the high arctic aerosol relevant for cloud formation. *Journal of Geophysical Research: Atmospheres*, **107 (D12)**, AAC–1.

Leck, C. and Persson, C., 1996a. The central Arctic Ocean as a source of dimethyl sulfide - seasonal variability in relation to biological activity. *Tellus B*, **48 (2)**, 156–177.

Leck, C. and Persson, C., 1996b. Seasonal and short-term variability in dimethyl sulfide, sulfur dioxide and biogenic sulfur and sea salt aerosol particles in the arctic marine boundary layer during summer and autumn. *Tellus B*, **48 (2)**, 272–299.

Leck, C. and Svensson, E., 2015. Importance of aerosol composition and mixing state for cloud droplet activation over the arctic pack ice in summer. *Atmospheric Chemistry and Physics*, **15 (5)**, 2545–2568.

Leck, C., Tjernström, M., Matrai, P., Swietlicki, E. and Bigg, K., 2004. Can marine micro-organisms influence melting of the arctic pack ice? *Eos, Transactions American Geophysical Union*, **85 (3)**, 25–32.

Mauritsen, T., Sedlar, J., Tjernström, M., Leck, C., Martin, M., Shupe, M., Sjogren, S., Sierau, B., Persson, P., Brooks, I. and Swietlicke, E., 2011. An Arctic CCN-limited cloud-aerosol regime. *Atmospheric Chemistry and Physics*, **11 (1)**, 165–173.

Nilsson, E.D. and Bigg, E.K., 1996. Influences on formation and dissipation of high arctic fogs during summer and autumn and their interaction with aerosol. *Tellus B*, **48 (2)**, 234–253.

Orellana, M. and Leck, C., 2015. *Biogeochemistry of marine dissolved organic matter*, Academic Press, chapter Marine Microgels, 451–472.

Orellana, M.V., Matrai, P.A., Leck, C., Rauschenberg, C.D., Lee, A.M. and Coz, E., 2011. Marine microgels as a source of cloud condensation nuclei in the high Arctic. *PNAS*, **108 (33)**, 13612–13617.

O′Sullivan, D., Adams, M., Tarn, M., Harrison, A., Vergara-Temprado, J., Porter, G., Holden, M., Sanchez-Marroquin, A., Carotenuto, F., Whale, T. et al., 2018. Contributions of biogenic material to the atmospheric ice-nucleating particle population in North Western Europe. *Scientific reports*, **8 (1)**, 13821.

Petters, M. and Wright, T., 2015. Revisiting ice nucleation from precipitation samples. *Geophysical Research Letters*, **42 (20)**, 8758–8766.

Reigstad, M., Carroll, J., Slagstad, D., Ellingsen, I. and Wassmann, P., 2011. Intra-regional comparison of productivity, carbon flux and ecosystem composition within the northern barents sea. *Progress in Oceanography*, **90 (1-4)**, 33–46.

Schnell, R. and Vali, G., 1975. Freezing nuclei in marine waters. *Tellus*, **27 (3)**, 321–323.

Schweiger, A. and Key, J., 1992. Arctic cloudiness. comparison of ISCCP-C2 and Nimbus-7 satellite-derived cloud products with a surface-based cloud climatology. *Journal of climate*, **5 (12)**, 1514–1527.

Sedlar, J., Tjernström, M., Mauritsen, T., Shupe, M.D., Brooks, I.M., Persson, P.O.G., Birch, C.E., Leck, C., Sirevaag, A. and Nicolaus, M., 2011. A transitioning arctic surface energy budget: the impacts of solar zenith angle, surface albedo and cloud radiative forcing. *Climate Dynamics*, **37 (7-8)**, 1643–1660.

Serreze, M.C., Holland, M.M. and Stroeve, J., 2007. Perspectives on the arctic's shrinking sea-ice cover. *Science*, **315 (5818)**, 1533–1536.

Sotiropoulou, G., Sedlar, J., Forbes, R. and Tjernström, M., 2016. Summer arctic clouds in the ecmwf forecast model: An evaluation of cloud parametrization schemes. *Quarterly Journal of the Royal Meteorological Society*, **142 (694)**, 387–400.

Sprenger, M. and Wernli, H., 2015. The LAGRANTO lagrangian analysis tool–version 2.0. *Geoscientific Model Development*, **8 (8)**, 2569–2586.

Stevens, R.G., Loewe, K., Dearden, C., Dimitrelos, A., Possner, A., Eirund, G.K., Raatikainen, T., Hill, A.A., Shipway, B.J., Wilkinson, J., Romakkaniemi, S., Tonttila, J., Laaksonen, A., Korhonen, H., Connolly, P., Lohmann, U., Hoose, C., Ekman, A.M.L., Carslaw, K.S. and Field, P.R., 2018. A model intercomparison of CCN-limited tenuous clouds in the high Arctic. *Atmospheric Chemistry and Physics*, **18 (15)**, 11041–11071.

Stumm, W. and Morgan, J.J., 1981. *Aquatic chemistry: an introduction emphasizing chemical equilibria in natural waters*. John Wiley & Sons.

Tjernström, M., Leck, C., Birch, C.E., Bottenheim, J.W., Brooks, B.J., Brooks, I.M., Bäcklin, L., Chang, R.Y.W., de Leeuw, G., Di Liberto, L., de la Rosa, S., Granath, E., Graus, M., Hansel, A., Heintzenberg, J., Held, A., Hind, A., Johnston, P., Knulst, J., Martin, M., Matrai, P.A., Mauritsen, T., Müller, M., Norris, S.J., Orellana, M.V., Orsini, D.A., Paatero, J., Persson, P.O.G., Gao, Q., Rauschenberg, C., Ristovski, Z., Sedlar, J., Shupe, M.D., Sierau, B., Sirevaag, A., Sjogren, S., Stetzer, O., Swietlicki, E., Szczodrak, M., Vaattovaara, P., Wahlberg, N., Westberg, M. and Wheeler, C.R., 2014. The Arctic Summer Cloud Ocean Study (ASCOS): overview and experimental design. *Atmospheric Chemistry and Physics*, **14 (6)**, 2823–2869.

Tjernström, M., Leck, C., Persson, P.O.G., Jensen, M.L., Oncley, S.P. and Targino, A., 2004. The summertime Arctic atmosphere: meteorological measurements during the Arctic Ocean Experiment 2001. *Bulletin of the American Meteorological Society*, **85 (9)**, 1305–1322.

Twomey, S., 1977. *Atmospheric Aerosols*. Developments in Atmospheric Science. Elsevier, New York, U.S.A.

van Pinxteren, D., Fomba, K.W., Mertes, S., Müller, K., Spindler, G., Schneider, J., Lee, T., Collett, J.L. and Herrmann, H., 2016. Cloud water composition during HCCT-2010: Scavenging efficiencies, solute concentrations, and droplet size dependence of inorganic ions and dissolved organic carbon. *Atmospheric Chemistry and Physics*, **16 (5)**, 3185–3205.

Vergara-Temprado, J., Miltenberger, A.K., Furtado, K., Grosvenor, D.P., Shipway, B.J., Hill, A.A., Wilkinson, J.M., Field, P.R., Murray, B.J. and Carslaw, K.S., 2018. Strong control of southern ocean cloud reflectivity by ice-nucleating particles. *Proceedings of the National Academy of Sciences*, **115 (11)**, 2687–2692.

Wex, H., Huang, L., Zhang, W., Hung, H., Traversi, R., Becagli, S., Sheesley, R.J., Moffett, C.E., Barrett, T.E., Bossi, R., Skov, H., Hünerbein, A., Lubitz, J., Löffler, M., Linke, O., Hartmann, M., Herenz, P. and Stratmann, F., 2019. Annual variability of ice-nucleating particle concentrations at different arctic locations. *Atmospheric Chemistry and Physics*, **19 (7)**, 5293–5311.

Whale, T.F., Murray, B.J., O'Sullivan, D., Wilson, T.W., Umo, N., Baustian, K.J., Atkinson,

J.D., Workneh, D. and Morris, G., 2015. A technique for quantifying heterogeneous ice nucleation in microlitre supercooled water droplets. *Atmospheric Measurement Techniques*, **8 (6)**, 2437–2447.

Wilson, T.W., Ladino, L.A., Alpert, P.A., Breckels, M.N., Brooks, I.M., Burrows, S.M., Carslaw, K.S., Huffman, J.A., Judd, C., Kilthau, W.P. et al., 2015. A marine biogenic source of atmospheric ice-nucleating particles. *Nature*, **525 (7568)**, 234.

Table 1: The operating and technical parameters of the mini-CWS.

| | |
|---|---|
| Inlet dimensions | 13 x 13 cm |
| Strand diameter | 0.560 mm |
| Number of rows | 6 |
| Number of strings per row | 44 |
| Fractional coverage per row | 0.174 |
| Sample flow speed | 1.4 $ms^{-1}$ |
| Angle of inclination | 35° |
| Weight | approx. 7 kg |

Table 2: Synopsis of findings from the inorganic composition and INP content as well as back-trajectory analysis of selected samples.

| Sample | Inorganic composition | | INP content | Back-trajectory analysis |
|---|---|---|---|---|
| 17 August | MSA/nss-$SO_4^{-2}$: | 0.38 | Sample was not considered | Originated over the MIZ in Greenland |
| | $NH_4^+$/nss-$SO_4^{-2}$: | 0.78 | because of contaminated | Sea |
| | $Cl^-/Na^+$: | 0.82 | handling blank | |
| 22 August | MSA/nss-$SO_4^{-2}$: | 0.24 | Below baseline | Originated over East Siberian Sea, |
| | $NH_4^+$/nss-$SO_4^{-2}$: | 0.62 | | precipitation before arrival at sampling |
| | $Cl^-/Na^+$: | 1.86 | | site |
| 25 August | MSA/nss-$SO_4^{-2}$: | 0.51 | High signal; heat | Three out four trajectories coming |
| | $NH_4^+$/nss-$SO_4^{-2}$: | 0.97 | sensitivity indicates | from Ellesmere Island, one from East |
| | $Cl^-/Na^+$: | 1.04 | biologically active INP | Siberian Sea |
| 11 September | MSA/nss-$SO_4^{-2}$: | 0.15 | Close to baseline | Only over the pack ice, no contact with |
| | $NH_4^+$/nss-$SO_4^{-2}$: | 1.29 | | open water, high above BL, high wind |
| | $Cl^-/Na^+$: | 0.95 | | speeds upwind of sampling site |

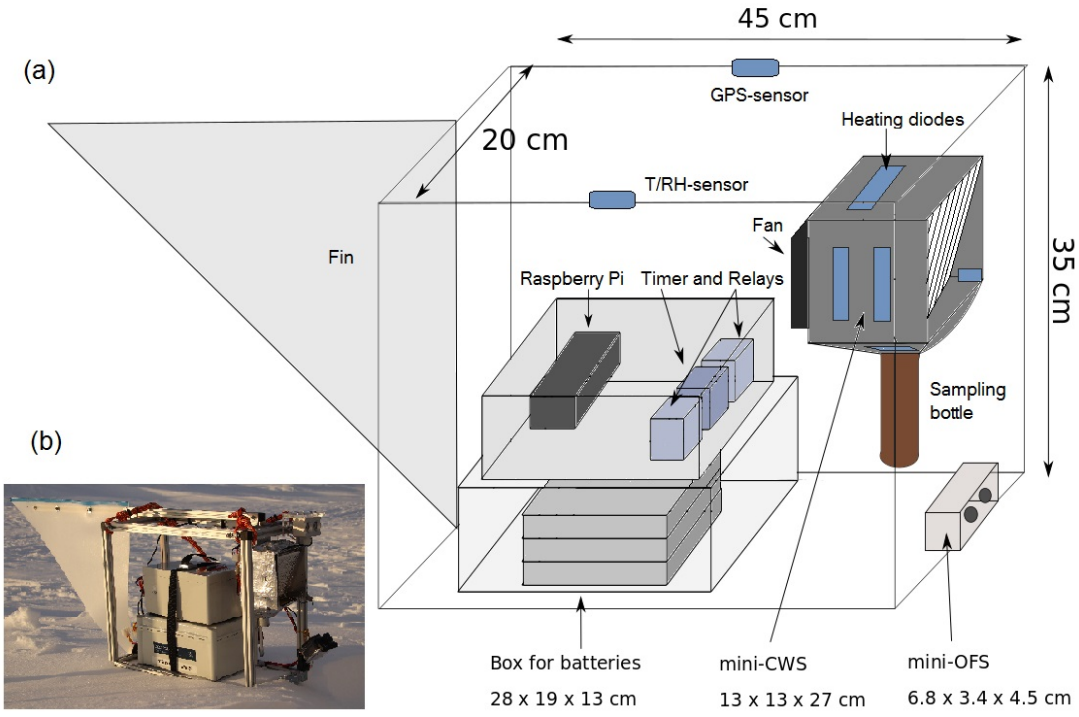


Figure 1: A schematic of the mini-CWS sampler. (a) The mini-CWS consists of the cloud water sampler unit, batteries, a data acquisition device, a timer with relays and sensors to measure temperature, humidity, visibility and GPS position. (b) Photo of the system prior to deployment in the high Arctic.

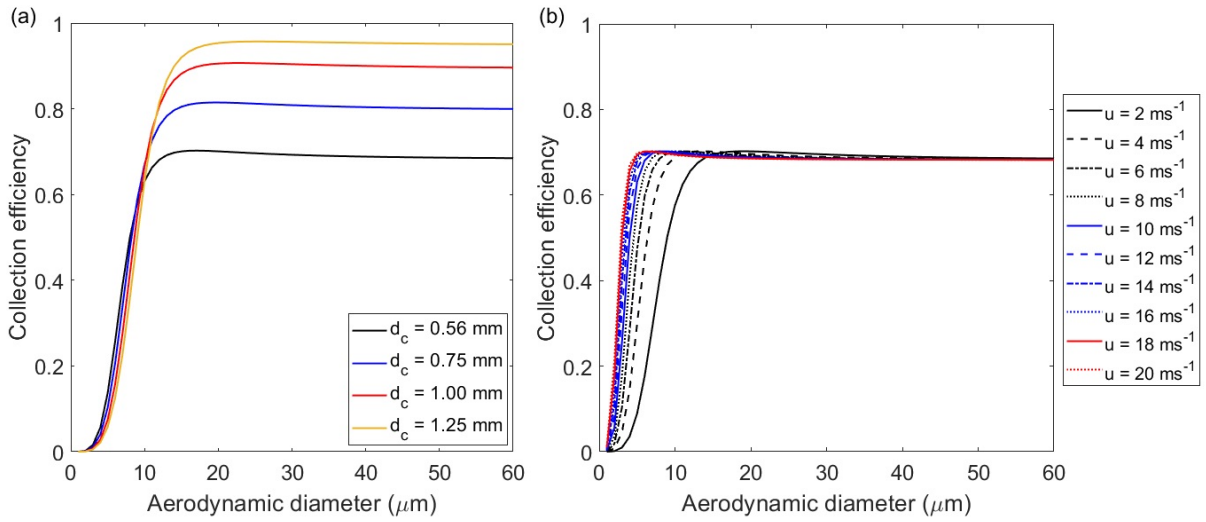


Figure 2: The theoretical collection efficiency of the mini-CWS. The collection efficiency is calculated according to the approach of Demoz et al. (1996) for (a) various strand diameters (the range of diameters presented here aim to include the effect of ice formation on the collection efficiency during sampling) and (b) various flow velocities.

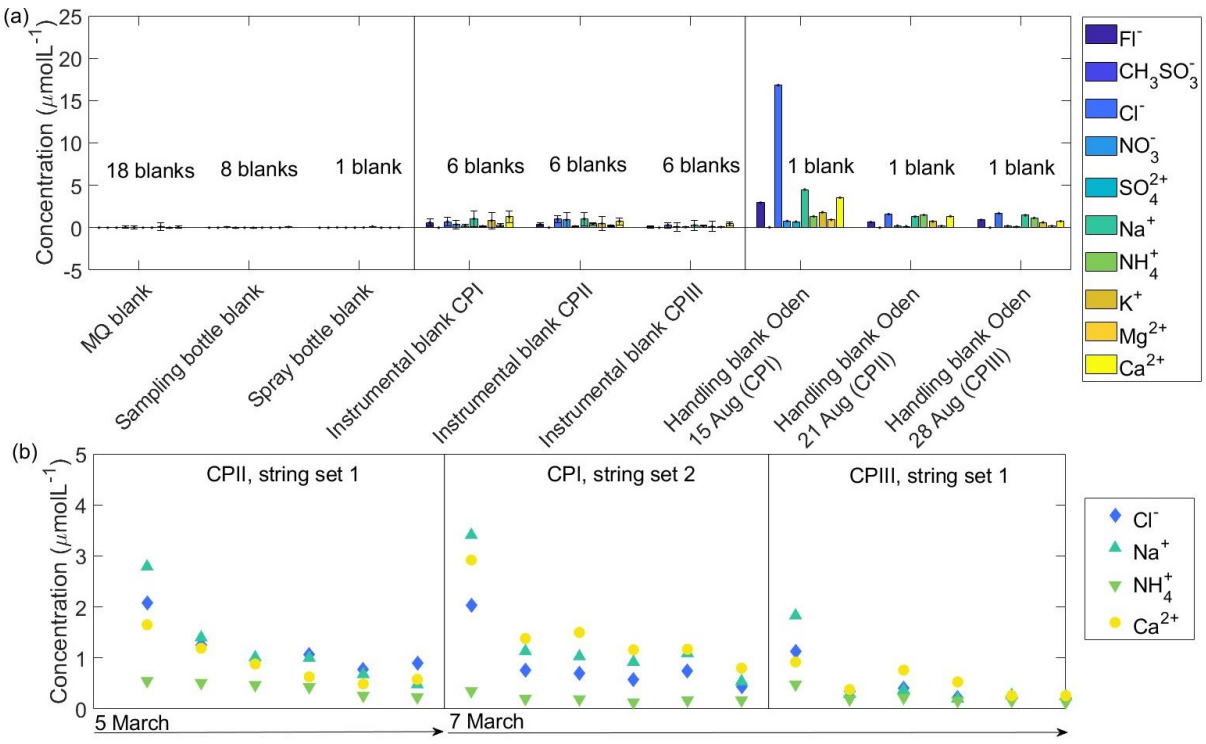


Figure 3: Comparison of blank samples. (a) Comparison of concentrations in three distinct handling blanks for different cleaning procedures (CP) that were taken during the expedition and mean concentrations in the reproduced blanks that were taken after the campaign as well as the mean concentrations from MQ blanks, sampling bottle blanks and a spray bottle blank. (b) Time series of concentrations in post-cruise instrumental blanks. Only a selected number of ions are shown for the sake of clarity. The timeseries for all analysed ions can be found in Figure S3 in the supplementary material.

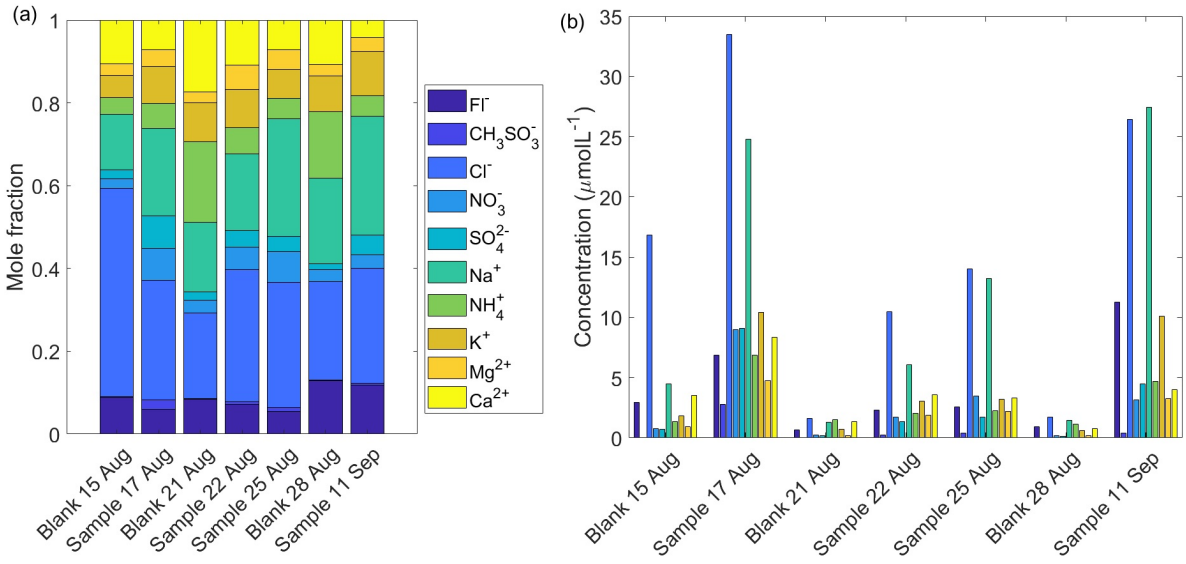


Figure 4: Mole fractions (a) and concentrations (b) of inorganic ions in different cloud water samples. Concentrations for non-blank corrected samples are compared to the concentrations measured in the handling blanks for the respective cleaning procedures.

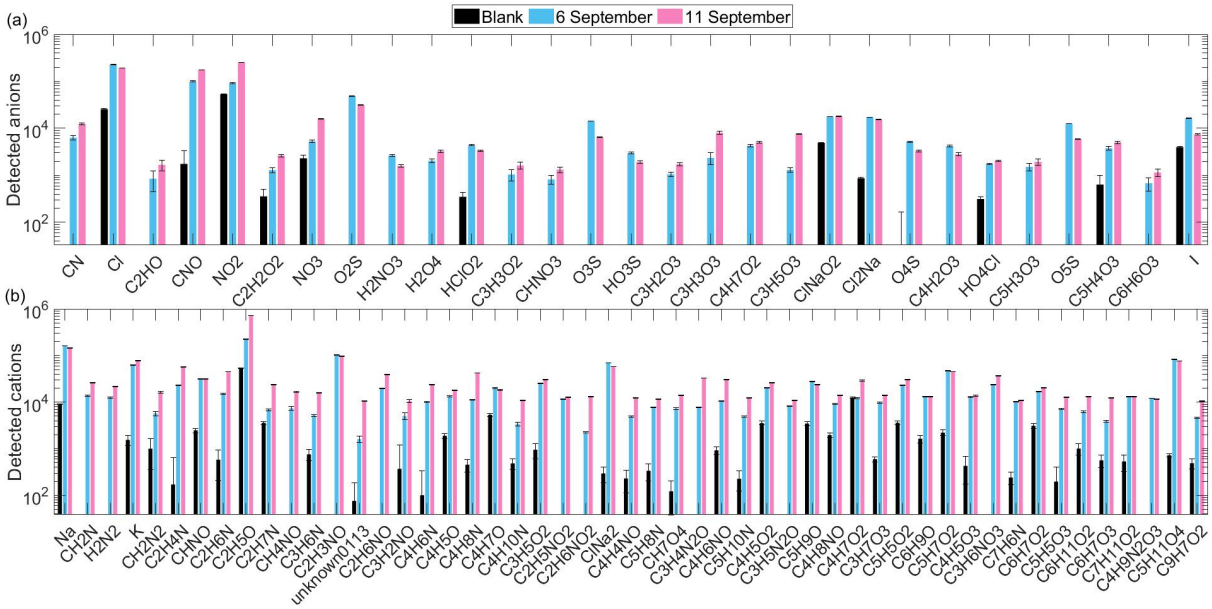


Figure 5: Mass spectrometer analysis (TDCIMS) of selected cloud water samples. Panel (a) displays the anions and panel (b) the cations detected in the samples collected on 6 and 11 September compared to the respective handling blank collected on the 28 August. Only anions with counts $\geq 1000$ and cations with counts $\geq 10000$ are displayed. When interpreting the results, one has to account for the dilution of the samples before they were run in negative mode.

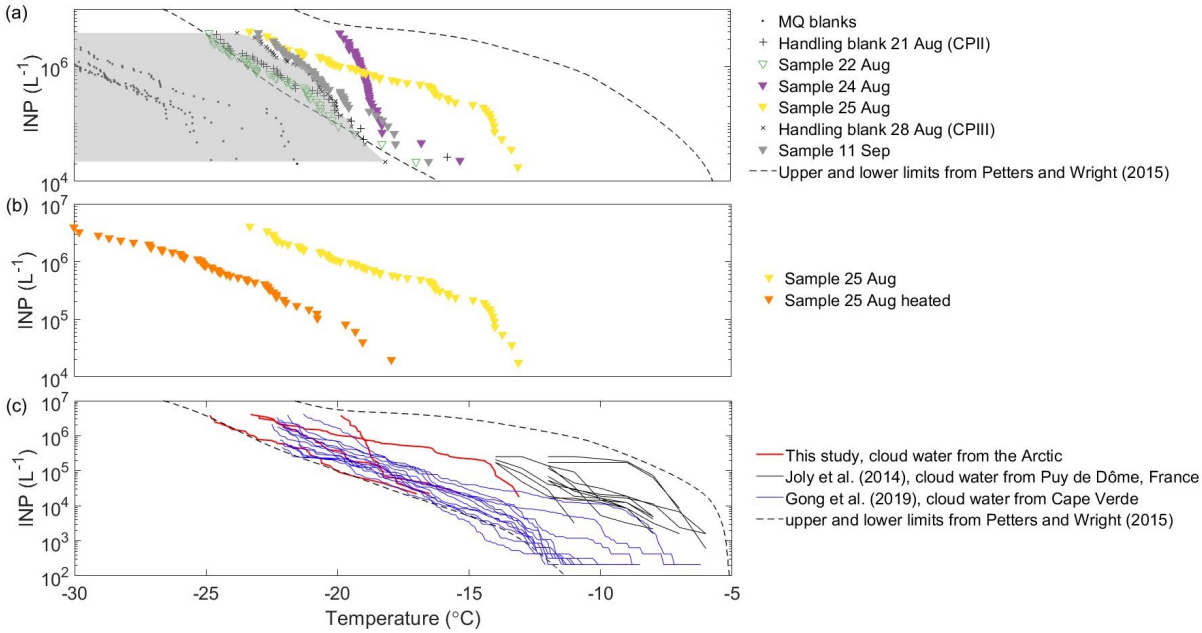


Figure 6: INP analysis of collected cloud water samples. (a) INP concentrations per litre of cloud water for collected samples, MQ blanks and handling blanks. The shaded area marks samples that fall below the baseline as set by the handling blanks. These samples are displayed with non-filled symbols and should be regarded as limiting values since they can not be discerned from the baseline. (b) Effect of heating on the sample collected on 25 August. (c) Comparison to INP concentrations in cloud water samples obtained from two different sampling sites.

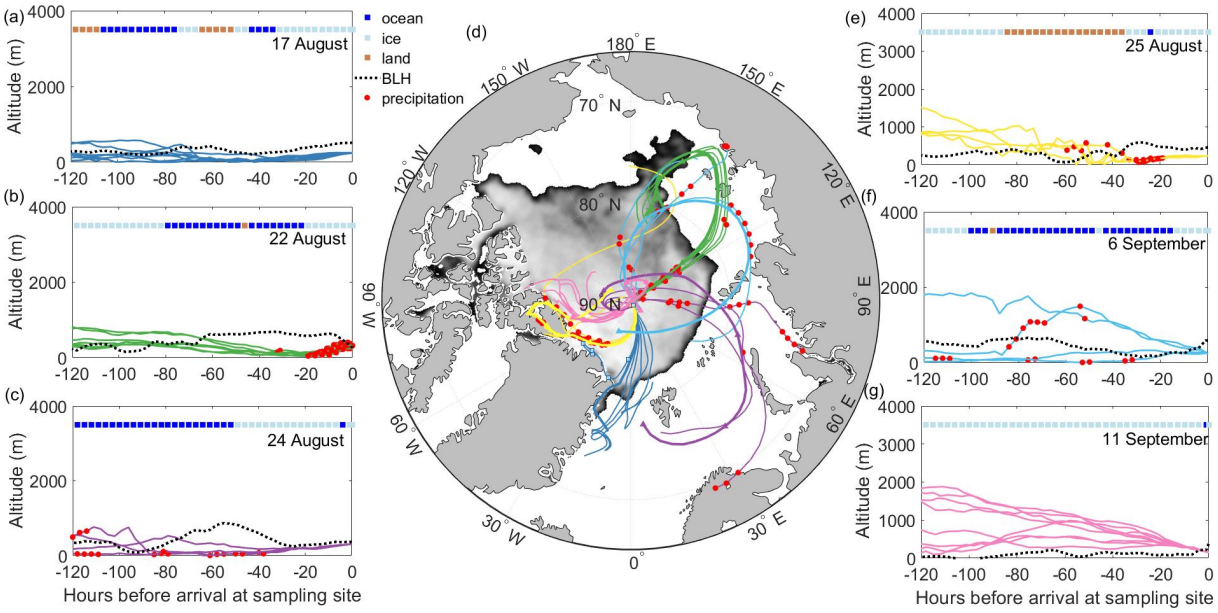


Figure 7: Hourly 5-day back trajectories for different cloud water samples. (a)-(c) and (e)-(g) vertical distribution of trajectories arriving at mean sampling altitude. Altitude is given in meters above sea level. Red dots mark precipitation if the amount of precipitation exceeded 0.1 mm per hour (threshold taken from Herenz et al., 2019). Time over ocean, ice and land is given for the mean trajectories. Time over ice was defined when the ice concentration exceeded 80%. Dotted line marks the height of the BL top (BLH). (d) Horizontal distribution of mean trajectories. Symbols mark every 24 hours. Sea ice edge is displayed for 11 September, data taken from the EUMETSAT Ocean and Sea Ice Satellite Application Facility (OSI SAF, www.osi-asf.org).

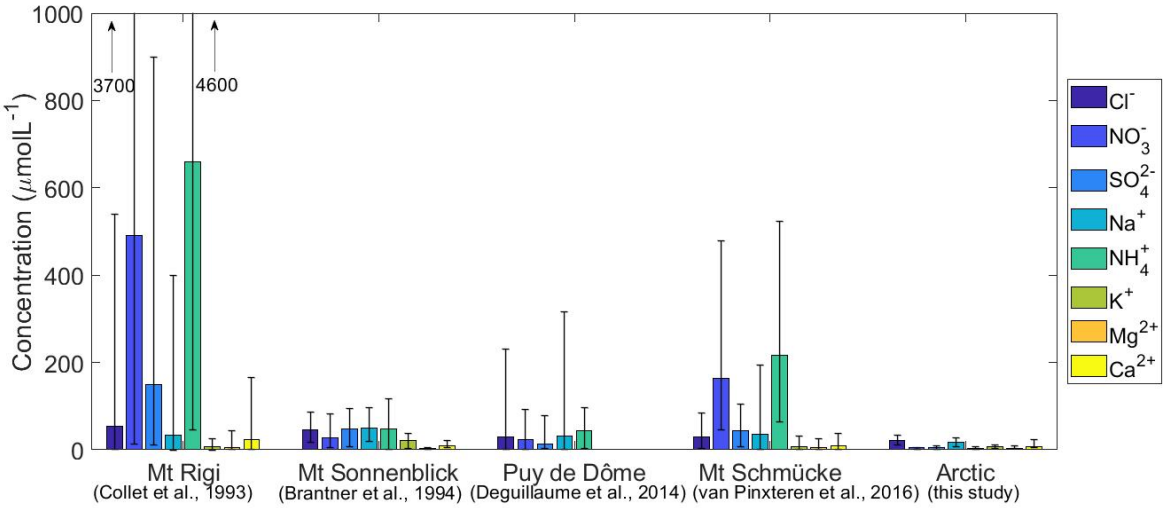


Figure 8: Comparison of cloud water composition obtained from different European sampling sites compared to this study. Mean values are given by coloured bars, black bars indicate the range.

## Supplementary material

Table S1: Cleaning protocol for the sampling bottles.

| Step | Procedure |
|---|---|
| 1 | Bottles were filled with a 5% solution of hydrochloric acid (HCl) and left for 24 hours |
| 2 | Two rinses with MQ-water |
| 3 | Three cycles in a lab-dishwasher |
| 4 | Rinsed with ethanol and left to dry |

Table S2: Cleaning procedures for mini-CWS and corresponding handling blanks.

| Procedure | Cleaning procedure | Comments |
|---|---|---|
| I | Strings UV irradiated; thoroughly rinsed with MQ water; MQ water sampled from spray bottle | Respective procedure for sample collected on 17 August |
| II | Strings bathed in ethanol; rinsed with MQ water; MQ water sampled from spray bottle | Respective procedure for sample collected on 22 August |
| III (final) | Strings bathed in ethanol; funnel cleaned with ethanol, clean room wipes and QTips; strings irradiated under UV (20 min each side); strings and funnel in ultrasonic bath of MQ water; MQ water sampled from spray bottle | Respective procedure for sample collected on 11 September |

Table S3: Concentration of inorganic ions in handling blank relative to concentrations in the obtained samples.

| Ratio blank : Sample | $Fl^-$ | $CH_3O_3S^-$ | $Cl^-$ | $NO_3^-$ | $SO_4^{2-}$ | $Na^+$ | $NH_4^+$ | $K^+$ | $Mg^{2+}$ | $Ca^{2+}$ |
|---|---|---|---|---|---|---|---|---|---|---|
| Blank 15 Aug : Sample 17 Aug | 0.43 | 0.01 | 0.50 | 0.09 | 0.08 | 0.18 | 0.19 | 0.18 | 0.20 | 0.42 |
| Blank 21 Aug : Median of samples 22 and 25 Aug | 0.27 | 0.029 | 0.13 | 0.09 | 0.11 | 0.14 | 0.70 | 0.24 | 0.10 | 0.39 |
| Blank 28 Aug : Sample 11 Sep | 0.08 | 0.02 | 0.06 | 0.07 | 0.02 | 0.05 | 0.25 | 0.06 | 0.06 | 0.19 |

Table S4: Sampling times and sample volumes for deployment on the balloon and overview of analysis performed on the cloud water samples.

| Date | Location | Sampling time | Time in cloud | Sample volume (mL) | Mean altitude (m) | Comments | Analysed with | | |
|---|---|---|---|---|---|---|---|---|---|
| | | | | | | | IC | IN | TDCIMS |
| 17 August 9:41 - 16:45 | 89.29°N 29.45°E | 7 h 4 min | 3 h | 25.7 | 267 | Deployment on balloon | X | X | |
| 22 August 9:46 - 16:50 | 89.32°N 7.53°E | 7 h 4 min | 49 min | 7.7 | 245, later raised to 412 | Deployment on balloon | X | X | |
| 24 August 9:54 - 14:24 | 89.31°N 15.36°E | 4 h 30 min | 2 h | 9.4 | 323 | Deployment on balloon | | X | |
| 25 August 11:00 - 16:00 | 89.32°N 22.12°E | 5 h | 27 min (probably longer) | 30.1 | 254 | Deployment on balloon batteries fully discharged at 13:30 | X | X | X |
| 6 September 19:00 - 22:10 | 88.54°N 46.15°E | 3 h 10 min | 2 h 21 min | 1.1 | 222 | Deployment on balloon | | | X |
| 11 September 11:30 - 19:30 | 88.38°N 45.06°E | 8 h | 1 h 29 min (certainly longer) | 12.1 | 374, sank to 180 | Deployment on balloon, battery fully discharged after 2 h | X | X | X |

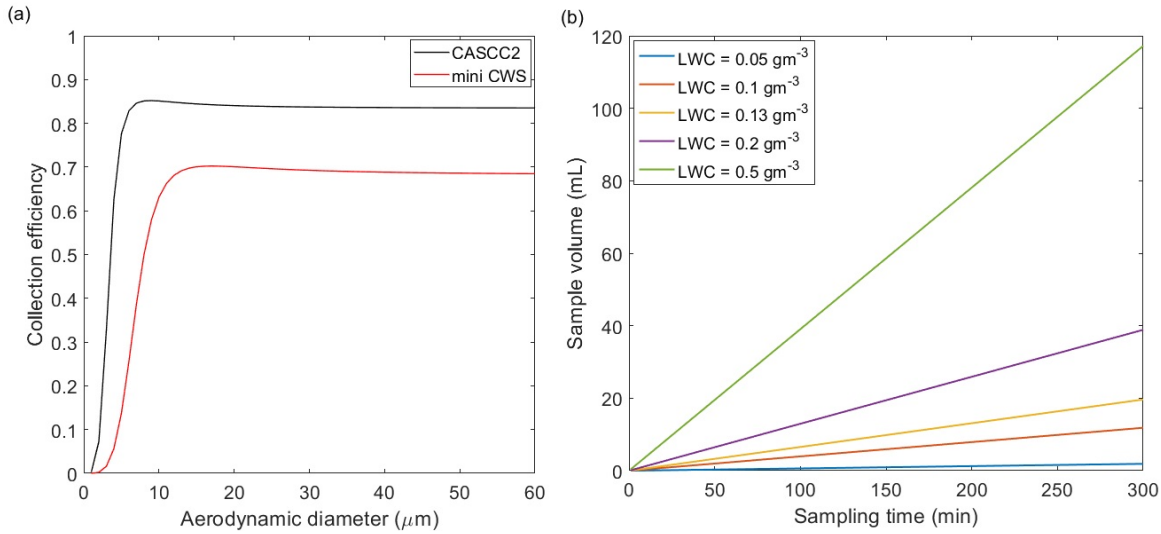


Figure S1: Comparison to CASCC2 and theoretically estimated sample volume. (a) Collection efficiency of the mini-CWS compared to the CASCC2 (Demoz et al., 1996) based on their respective sampling velocities (1.4 ms$^{-1}$ for the mini-CWS and 8.5 ms$^{-1}$ for the CASCC2) and (b) theoretically estimated sample volume for different LWCs.

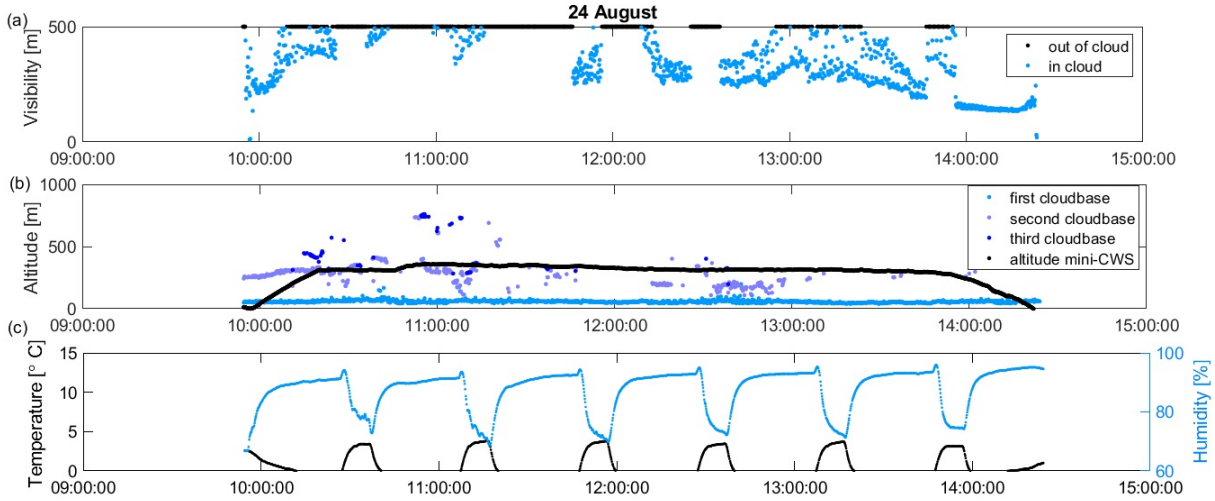


Figure S2: Data recorded by the sensors during deployment for 24 August 2018. (a) Timeline of measured visibility, (b) measured altitude and cloud base heights from ceilometer measurements as well as (c) monitored heating-sampling cycle and relative humidity.

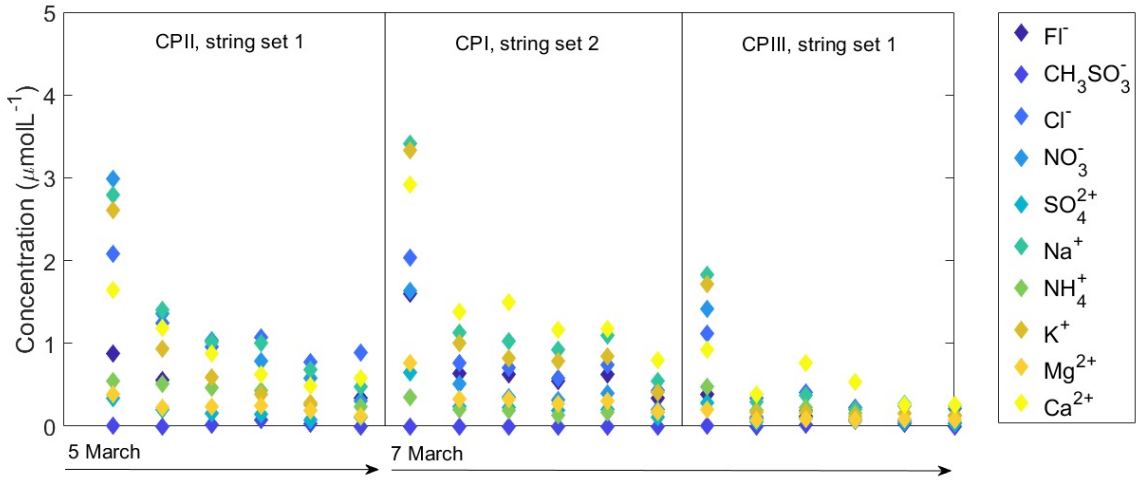


Figure S3: Timeseries of concentrations in post-cruise instrumental blanks for all cleaning procedures (CP) and all inorganic ions. For discussion see Section 3.1.

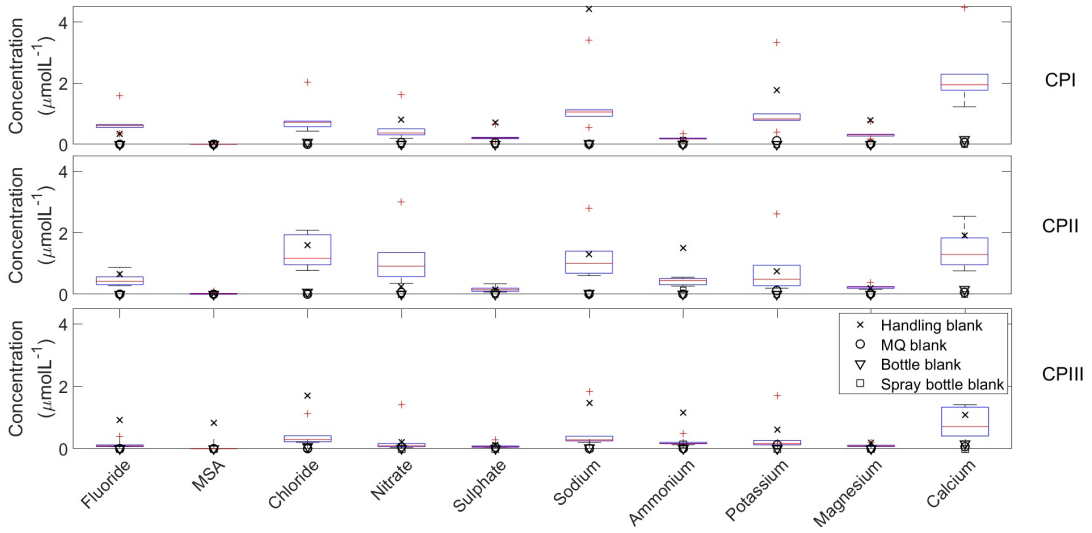


Figure S4: Comparison of instrumental and handling blanks. Boxplot of instrumental blanks for the different cleaning procedures compared to the concentrations in the handling blanks (black crosses). Red crosses are outliers of the instrumental blanks.